Journal of New Materials for Electrochemical Systems 17, 225-230 (2014)

Low Resistance, Carbon Black-free Magnetite Anode for Li-ion Batteries Obtained by One-step Attachment of Carbon Nanotubes

P. Półrolniczak[1], A. Arunthathy Surendran[1,2], M. Walkowiak[1,*], S. Thomas[2] and A.M. Stephan[3]

[1]Institute of Non-Ferrous Metals Division in Poznań Central Laboratory of Batteries and Cells, Forteczna 12 St., 61-362 Poznań, Poland
[2]Centre for Nanoscience and Nanotechnology, Mahatma Gandhi University, Kottayam, Kerala, India 686 560
[3]Central Electrochemical Research Institute, Electrochemical Power Systems Division, Karaikkudi 630006, Tamil Nadu, India

Received: May 27, 2014, Accepted: September 26, 2014, Available online: November 25, 2014

Abstract: *The paper describes a simple, one-step synthetic route for the fabrication of nanometric iron (III) oxide attached to multi-walled carbon nanotubes (MWCNT). TEM images show that magnetite nanoparticles with primary particle sizes of ca. 10 nm are preferentially located on the outer walls of carbon nanotubes. The obtained nanocomposites have been examined on reversible electrochemical insertion of lithium cations in a Li-ion cell. The presence of MWCNT brings about a substantial increase of the magnetite reversible capacities in the absence of any additional carbonaceous conductivity enhancing agent. With increasing MWCNT content in the material, reversible capacity consistently rises from 207 mAhg^{-1} for pure iron (III) oxide up to 763 mAhg^{-1} for the composite with 40 % of MWCNT. Cyclic voltammetry measurements reveal the expected large hysteresis between the reduction and oxidation peaks associated with Li^+ insertion/deinsertion into magnetite crystal lattice. The reductive current peak maxima steadily rise with increasing MWCNT content from 0.15 A g^{-1} for pure iron (III) oxide up to 0.4 A g^{-1} for the composite with 40 % of MWCNT which confirms faster kinetics of electrochemical processes. EIS measurements directly proved the internal resistance decrease connected with the incorporation of MWCNT.*

Keywords: Li-ion batteries; Fe_3O_4; magnetite; multi-walled carbon nanotubes

1. INTRODUCTION

Increasing demand for high performance electrochemical energy storage devices observed in the last years has been stimulating extensive research in the field of novel lithium ion battery materials. As far as anode materials are concerned, graphite is today by far the most frequently applied type of material in spite of their widely known limitations such as moderate specific capacity, sluggish solid state lithium cation mobility and inherent incompatibility with some electrolyte compositions. In contrast to graphite, certain transition metal oxides are known to deliver significantly higher reversible Li storage capacities (500-1000 mAh g^{-1}) [1-3]. Transition metal oxides such as Co_3O_4 [4], MnO_2 [5], MoO_3 [6], Fe_2O_3 [7] and Fe_3O_4 [8-10] have demonstrated promising electrochemical behavior. Most of metal oxides are known to adopt the so-called conversion mechanism to store reversibly a large amount of Li^+ ions, in contrast to intercalation-type mechanism occurring in graphitic structures. During the discharge metal oxides are reduced to the metallic state embedded in the Li_2O matrix. Upon charging Li_2O decomposition and Li^+ removal occurs accompanied by metal oxidation [11]. Among transition metal oxides, Fe_3O_4 (magnetite) has been considered as potentially one of the most attractive Li-ion anode materials due to its high theoretical capacity (926 mAh g^{-1}), high conductivity, environmental friendliness, low cost and natural abundance [12-14]. However, like other oxides, Fe_3O_4 also suffers from severe volume changes during repeated charge/discharge processes, which lead to particle cracking, electrode pulverization and subsequent loss of electrical contact between the electrode and the current collector [15]. Great efforts have been made to alleviate this fundamental problem, however with only limited success. One possible strategy is to produce nanometer-scale particles. There has been only partial success in nanostructured Fe_3O_4 electrode manufacturing having satisfactory reversible capacity and cyclic stability [16, 17]. An-

*To whom correspondence should be addressed:
Email: marusz.walkowiak@claio.poznan.pl
* ISE member

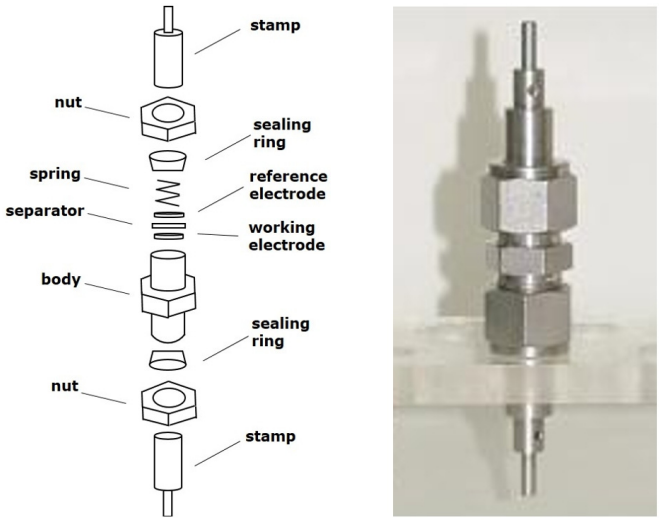

Figure 1. Exploded view drawing (left) and photo image (right) of Swagelok type cell.

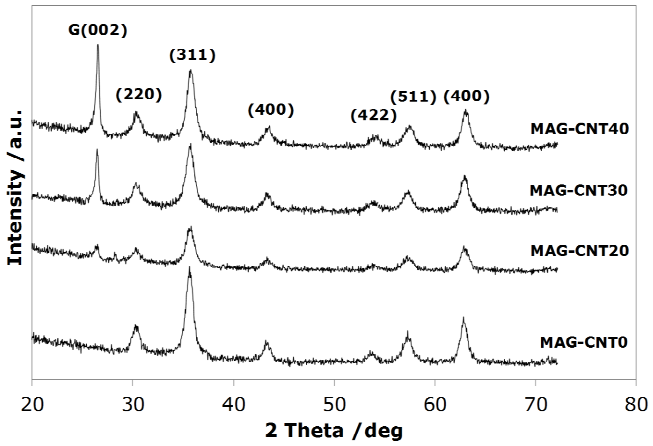

Figure 2. XRD patterns of Fe_3O_4/MWCNT nanocomposites and pure magnetite; G at the Miller index stands for graphite phase.

other approach is to prepare a composite of iron oxide with a carbon compounds. Examples are Fe_3O_4 nanospheres co-synthesized with carbon matrix [18] or carbon-coated Fe_3O_4 nanostructures [19, 20]. Very recent reports refer to Fe_3O_4 nanoparticles anchored/bonded to graphene [21-24] or carbon nanotubes [25, 26] (however without application in Li-ion batteries). It is generally believed that carbonaceous component acts as a structural buffer to accommodate mechanical stress caused by volume change during charge/discharge process, at the same time preserving good electronic conductivity of the electrode [27]. Recently, Dillon et al. have fabricated Li-ion anode based on a nanostructured Fe_3O_4/SWCNT composite [28]. However, the production of pure single walled carbon nanotubes is very expensive and difficult to scale up which is unfavorable for wider application in Li-ion batteries.

Herein we report easy, one-step solvothermal synthesis of Fe_3O_4 nanocomposite with multi-walled carbon nanotubes having favorable electrochemical characteristics.

2. EXPERIMENTAL

Fe_3O_4 (magnetite) and Fe_3O_4/MWCNT nanocomposites have been obtained by a solvothermal synthetic route. The multi-walled carbon nanotubes (MWCNT, purchased from Aldrich, product number 659258, MWCNT content ≥ 90 %, diameter = 110 – 170 nm, length = 5 - 9 μm) were first dispersed in a solvent mixture comprising 60 ml of ethylene glycol, 30 ml of tetraethylene glycol and 30 ml of H_2O, followed by stirring for 2 h to form a homogeneous suspension. 0.25 g of $FeCl_3 \cdot 6H_2O$ was subsequently added to the reaction bath. Finally, NaOH (0.29 g) was added as precipitating agent. After stirring for 2 h, the mixture was transferred to a Teflon-lined stainless steel autoclave and subjected to reaction at 180°C for 24 h. The final product was centrifuged and washed consecutively with distilled water and ethanol. Three Fe_3O_4/MWCNT composites have been obtained having calculated MWCNT contents: 20, 30 and 40% (samples MAG-CNT20, MAG-CNT30 and MAG-CNT40, respectively). Pristine Fe_3O_4 was also synthesized by the same procedure but in the absence of carbon nanotubes (sample MAG-CNT0).

The phase structure of the obtained powders was determined by X-ray diffraction (XRD) technique with the application of Philips PW 1050 diffractometer with CuK_α irradiation (λ = 0.154056 nm). Texture and morphology of the synthesized materials were examined by means of scanning (SEM) and transmission (TEM) electron microscopy techniques using Zeiss EVO 40 (SEM) and JOEL JEM 1200 EX (TEM) instruments. Actual elemental carbon content was determined using VarioMicro Elemental Analyser.

The electrodes for the electrochemical tests have been prepared by casting the slurry containing the active material onto a copper current collector. The slurry consisted of 90 wt.% Fe_3O_4 or Fe_3O_4/MWCNT nanocomposite and 10 wt.% PVdF (polyvinylidene fluoride, Fluka) as binder. The electrodes have been tested in Swagelok-type cells (see Fig. 1) with metallic lithium as counter and reference electrode and a conventional lithium-conducting electrolyte consisting of 1M $LiPF_6$ solution in EC/DMC, where EC – ethylene carbonate and DMC – dimethyl carbonate. The cells were galvanostatically charged/discharged at a current density of 10 mA g^{-1} between 0 and 3 V versus Li^+/Li. Typically ten complete galvanostatic cycles were performed. Potentiodynamic tests were performed at the scanning rate of 0.05 mV s^{-1} between 0 and 3 V. The electrochemical impedance spectroscopy measurements were carried out in the frequency region from 500 kHz to 10 mHz by applying the signal amplitude of 10 mV. All electrochemical measurements were carried out using multichannel VMP3 potentiostat/galvanostat (Bio-Logic).

3. RESULTS AND DISCUSSION

Fig. 2 shows XRD patterns of the synthesized magnetite-MWCNT composites with pure magnetite sample (MAG-MWCNT0) as the reference. The diffraction peak at 26.5 °2Θ is ascribed to the graphitic (002) reflection of MWCNT. Intensity of this signal obviously increases with the increase of MWCNT content. The (004) reflection partly overlaps with the magnetite (442) peak. High ratio of graphitic staking order is an inherent character-

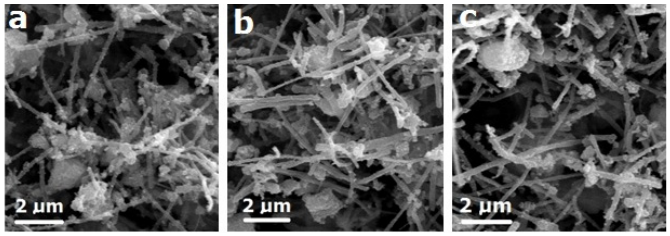

Figure 3. Scanning electron microscopy images of Fe_3O_4/MWCNT composites: (a) sample MAG-MWCNT20 b) sample MAG-MWCNT30 c) sample MAG-MWCNT40.

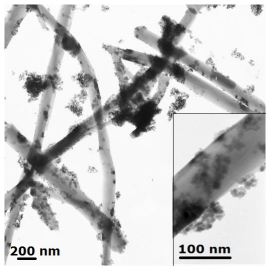

Figure 4. Typical transmission electron microscopy images of a magnetite-MWCNT composite.

istic of this product. Diffraction peaks in the range of 30-70° 2Θ match well with the (220), (311), (400), (422), (511) and (400) reflections of the standard fcc phase of magnetite. Significant broadening of diffraction peaks suggests small crystallite dimensions along all crystallographic axes.

Actual elemental carbon content was determined for the synthesized Fe_3O_4/MWCNT nanocomposites and the results are presented in Table 1 along with the calculated/planned values. As can be seen, the actual values are very close to the expected ones. Inevitable differences result from the fact that small fraction of the oxide is lost upon separation of the product from the reaction solution.

Figs. 3 and 4 show SEM and TEM images of the composite materials, respectively. As can be seen, vast part of magnetite is located onto the carbon nanotubes. Actual location of magnetite nanoparticles and their dispersion is of great importance as far as the resultant overall conductivity is concerned. In this respect, magnetite agglomerates existing in separation from the nanotubes are unfavorable, whereas the situation where single magnetite nanoparticles are attached to the outer nanotube walls should provide good conditions for both electronic and ionic transport. In the obtained materials, certain portion of Fe_3O_4, impossible to determine precisely,

Table 1. Carbon content measured for Fe_3O_4/MWCNT nanocomposites.

Sample designation	Calculated MWCNT content / %	Actual elemental carbon content / %
MAG-CNT0	0	0
MAG-CNT20	20	22
MAG-CNT30	30	32
MAG-CNT40	40	41

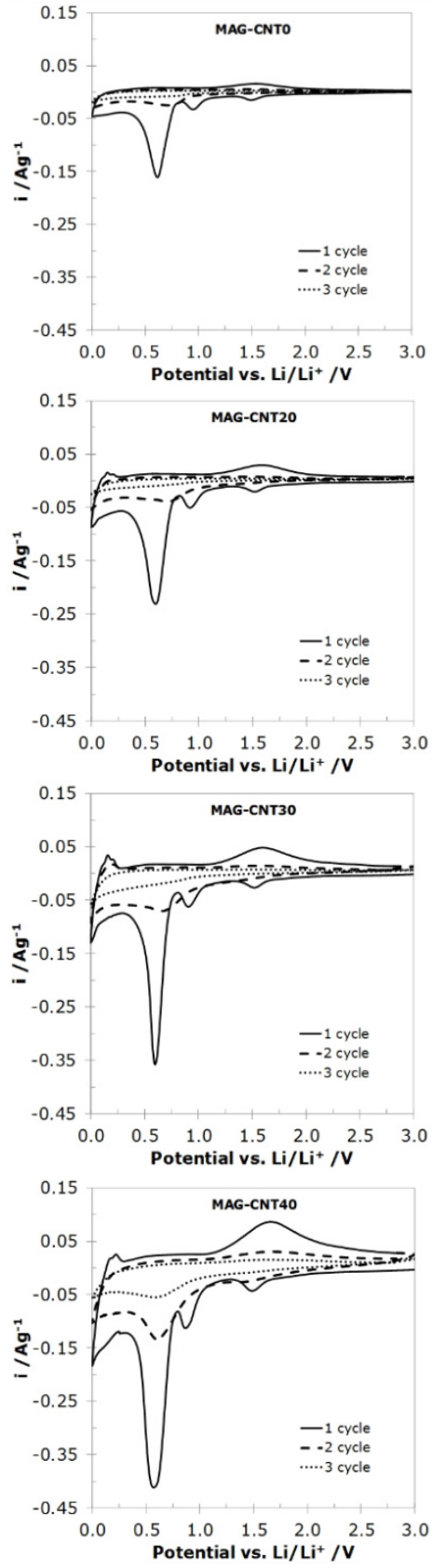

Figure 5. Cyclic voltammetry curves for the first 3 cycles for the Fe_3O_4/CNT nanocomposites.

forms unwanted agglomerates with poor contact with nanotubes but it seems that the majority of it is well distributed along the nanotube walls. This is particularly visible on TEM images where individual magnetite nanoparticles can clearly be seen.

Electrochemical lithium cation insertion into magnetite-MWCNT composites have been studied by means of cyclic voltammetry technique versus Li/Li^+ reference electrode, at a scan rate of 0.05 mV s^{-1} (Fig. 5). In the first cycle, pure magnetite electrode (Fig. 5a) exhibits two irreversible peaks with maxima at ca. 1.6 V and 0.9 V associated with solid electrolyte interphase formation which disappear in the subsequent cycles and the main reversible peak at ca. 0.6 V which has its broad counterpart on the oxidative part of the curve at ca. 1.6 V. This pair of current peaks must be attributed to the main reversible process involving reversible transition from Fe^{3+} to Fe^{2+} and further to Fe^0, accompanied by the formation of Li_2O. The presence of MWCNT brings about substantial corrections to the CV characteristics. Although the typical pattern of magnetite electrode is preserved in terms of the current peaks potentials, the observed current densities are strikingly higher as compared to pure Fe_3O_4 electrode. Taking into account the main reversible reduction peak at 0.6 V, the peak current density rises from 0.16 Ag^{-1} for pure magnetite (Fig. 5a) to 0.23 Ag^{-1} for the composite with 20% of MWCNT (Fig. 5b) and further consistently increases to 0.36 Ag^{-1} and 0.42 Ag^{-1} for 30% and 40% of MWCNT, respectively. The observed rise of current signals must be attributed to an enhancement of kinetic conditions of electrochemical processes connected to the presence of effective conducting network formed by the nanotubes. What is characteristic, the CV curves of materials containing MWCNT feature clear current signals near 0 V associated with reversible lithium cation intercalation into the traces of graphitic crystal lattice, with the possibility to even distinguish intercalation stages. MWCNT as such do not give any well distinguishable current signals. An unfavorable information that can be further read out from the CV curves is that the current peaks quickly decrease upon the second and third cycle. Closer inspection allows for a cautious observation that the capacity fade is less pronounced for the materials with the highest nanotube content. Thus, although MWCNT proved to be effective in enhancing the transport conditions, the problem of detrimental structure changes remains largely unresolved.

Galvanostatic experiments allow for the determination of exact specific capacities and for a closer insight into the issue of capacity fade upon cycling. Fig. 6 presents charge/discharge curves in the first cycles recorded at the current density of 10 mAg^{-1}. In the insets, plots of discharge capacities during 10 cycles have been shown. Table 2 contains numerical data obtained from galvanostatic experiments. As can be seen, MWCNT causes dramatic improvement of such key parameters as discharge capacity (reversible capacity), irreversible capacity and coulombic efficiency in the first cycle. Coulombic efficiencies in the subsequent cycles are stable and are generally in the range of 90-92%, without clear correlation with the electrode composition. The differences among 20, 30 and 40% of MWCNT are not as important as between these three samples and pure Fe_3O_4 but the electrodes performance generally tends to improve with increasing MWCNT content. Reversible capacity reaches optimal value of 763 $mAhg^{-1}$ for the composite with 40% of MWCNT which is more than twice as much as for graphites. Upon subsequent several cycles capacity of pure magnetite drops in

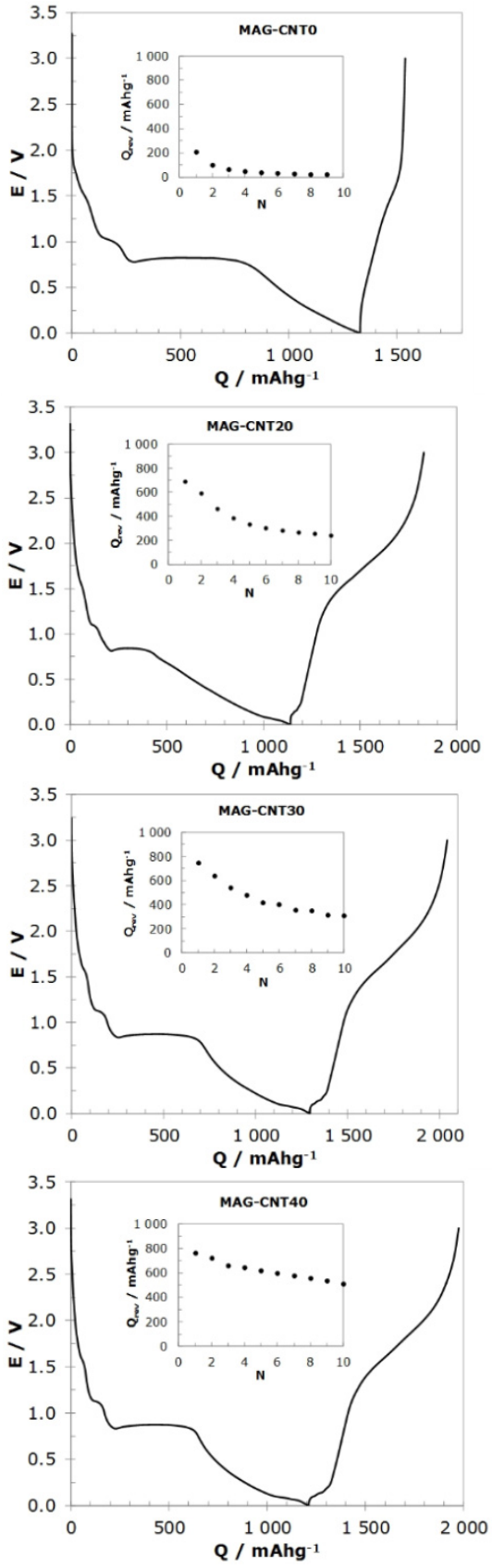

Figure 6. Charge/discharge profiles for the Fe_3O_4/CNT nanocomposites (inset cyclic stability).

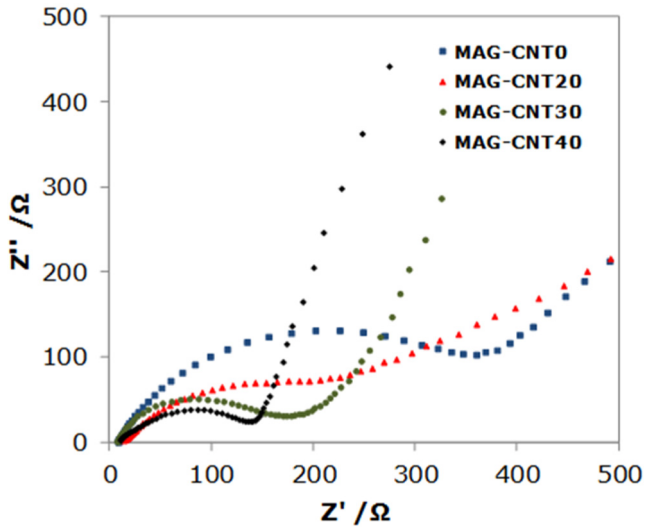

Figure 7. Nyquist plots of Fe_3O_4/CNT nanocomposites and pure Fe_3O_4 after 3 galvanostatic charge/discharge cycles.

practice to zero, whereas samples containing MWCNTs continue to deliver substantial amounts of charge. The rate of capacity fade is still fast but the progress is significant especially for the sample with 40% of MWCNTs (Fig. 6d) which delivers over 500 $mAhg^{-1}$ even after 10 cycles.

The obtained magnetite-based anode materials are thus characterized by enhanced charge transfer properties as a result of favorable interconnection between active magnetite nanoparticles and the conductive network composed of nanotube filaments. This claim should be verifiable through the determination of the electrodes impedance responses. Fig. 7 depicts Nyquist plots obtained after 3 charge/discharge cycles. The patterns exhibit well known semicircles, the diameters of which are attributable to the charge transfer resistances. Table 2 contains the corresponding R_{LF} parameters (resistances associated with the low frequency semicircles). Together with increasing MWCNT content the charge transfer resistances markedly decrease, suggesting facilitated ionic transport from the near-electrode into the bulk of the magnetite lattice. The size of Fe_3O_4 particles is reduced to approximately 10 nm, therefore active surface area is large and acceleration of the Li-ion diffusion and reaction with metal oxide is achieved. Furthermore, the MWCNT network on which Fe_3O_4 nanoparticles are anchored serves as flexible electronic pathway for a rapid charge transfer which manifests as reduced electrode resistance.

4. CONCLUSIONS

The applied synthesis method allowed for obtaining a composite material consisting of magnetite nanoparticles well dispersed and preferentially attached to the outer walls of multi-walled carbon nanotubes. Fe_3O_4 is the active component in the composite material, contributing to the charge storage, whereas carbon nanotubes provide electronically conducting network. Uniqueness of the presented approach is based on the fact that, unlike in similar other works, no additional carbon conducting agent has been added to the electrode. The materials function effectively in terms of reversible lithium cation insertion which has been evidenced by means of cyclic voltammetry and galvanostatic technique. With increasing nanotubes content current peaks on the CV curves and reversible capacities increase up to 763 $mAhg^{-1}$ for the most MWCNT-rich material. Cyclic stability significantly enhances with MWCNT content, suggesting that volume changes associated with repeated charging have to some extent been alleviated, although in practical terms the issue of cyclic stability requires further consideration. A unique combination of nanometric magnetite particles with highly conducting MWCNT network gave rise to markedly reduced electrode internal resistance which has been evidenced by EIS measurements. From the technological point of view the study demonstrates that MWCNT alone is capable of providing effective conducting matrix for the active insertion material, thus eliminating the costly and energy consuming operations associated with incorporation of an additional conducting agent.

5. ACKNOWLEDGEMENTS

This work has been financially supported by the National Science Centre of Poland, grant No UMO-2011/03/B/ST5/01508.

REFERENCES

[1] A.S. Arico, P. Bruce, B. Scrosati, J.M. Tarascon, W. Van Schalkwijk, Nat. Mater., 4, 366 (2005).
[2] Y.S. Hu, Y.G. Guo, W. Sigle, S. Hore, P. Balaya, J. Maier, Nat. Mater., 5, 713 (2006).
[3] P. Poizot, S. Laruelle, S. Grugeon, L. Dupont, J.M. Tarascon, Nature, 407, 496 (2000).
[4] J. Liu, Y.L. Wan, C.P. Liu, W. Liu, S.M. Ji, Y.C. Zhou, J.B. Wang, Eur. J. Inorg. Chem., 24, 3825 (2012).
[5] H. Xia, M. Lai, L. Lu, J. Mater. Chem., 20, 6896 (2010).
[6] S.-H. Lee, Y.-H. Kim, R. Deshpande, P.A. Parilla, E. Whitney, D.T. Gillaspie, K.M. Jones, A.H. Mahan, S. Zhang, A.C. Dillon, Adv. Mater., 20, 3627 (2008).
[7] Y.-M. Lin, P.R. Abel, A. Heller, C.B. Mullins, J. Phys. Chem.

Table 2. Electrochemical parameters for Fe_3O_4/CNT nanocomposites and pure Fe_3O_4 (Q_{1ch} – charge capacity in the 1st cycle, Q_{1dis} – discharge capacity in the 1st cycle, Q_{irr} – irreversible capacity, E_{ff} – coulombic efficiency of charging in the 1st cycle, R_{LF} – low-frequency resistance).

Sample	$Q_{1ch.}$ / $mAhg^{-1}$	$Q_{1\ disch.}$ / $mAhg^{-1}$	Q_{irr} / $mAhg^{-1}$	E_{ff} / %	R_{LF} / Ω
MAG-CNT0	1537	207	1330	14	459
MAG-CNT20	1139	690	449	60	360
MAG-CNT30	1294	747	547	58	186
MAG-CNT40	1210	763	447	63	157

Lett., 22, 2885 (2011).
[8] Z. Xiao, Y. Xi, Z. Ren, Z. Liu, G. Xu, C. Chao, X. Li, G. Shen, G. Han, J. Mater. Chem., 22, 20566 (2012).
[9] D. Su, H.-J. Ahn, G. Wang, J. Power Sources, 244, 742 (2013).
[10]S. Wang, J. Zhang, C. Chen, J. Power Sources, 195, 5379 (2010).
[11]Z.M. Cui, L.Y. Jiang, W.G. Song, Y.G. Guo, Chem. Mater., 21, 1162 (2009).
[12]X. Zhu, W. Wu, Z. Liu, L. Li, J. Hu, H. Dai, L. Ding, K. Zhou, Ch. Wang, X. Song, Electrochim. Acta, 95, 24 (2013).
[13]W.-M. Zhang, X.-L. Wu, J.-S. Hu, Y.-G. Guo, L.-J. Wan, Adv. Funct. Mater., 18, 3941 (2008).
[14]L. Taberna, S. Mitra, P. Poizot, P. Simon, J.M. Tarascon, Nat. Mat., 5, 567 (2006).
[15]J.Z. Wang, C. Zhong, D. Wexler, N.H. Idris, Z.X. Wang, L.Q. Chen, H.K. Liu, Chem. Eur. J., 17, 661 (2011).
[16]H. Duan, J. Gnanaraj, X. Chen, B. Li, J. Liang, J. Power Sources, 185, 512 (2008).
[17]S.K. Behera, J. Power Sources, 196, 8669 (2011).
[18]J.S. Chen, Y.M. Zhang, X.W. Lou, ACS Appl. Mater., Interfaces 3, 3276 (2011).
[19]Q.Q. Xiong, Y. Lu, X.L. Wang, C.D. Gu, Y.Q. Qiao, J.P. Tu, J. Alloy. Compd., 536, 219 (2012).
[20]S. Yuan, Z. Zhou, G. Li, Cryst. Eng. Comm., 13, 4709 (2011).
[21]X. Huang, X. Zhou, K. Qian, D. Zhao, Z. Liu, Ch. Yu, J. Alloy. Compd., 514, 76 (2012).
[22]Y. Ch. Dong, R.G. Ma, M.J. Hu, H. Cheng, Ch.K. Tsang, Q.D. Yang, Y.Y. Li, J.A. Zapien, J. Solid State Chem., 201, 330 (2013).
[23]G. Zhou, D.-W. Wang, F. Li, L. Zhang, N. Li, Z.-S. Wu, L. Wen, G.Q. Lu, H.-M. Cheng, Chem. Mater., 22, 5306 (2010).
[24]M. Sathish, T. Tomai, I. Honma, J. Power Sources, 217, 85 (2012).
[25]N. Zhao, S. Wu, Ch. He, Z. Wang, Ch. Shi, E. Liu, J. Li, Carbon, 57, 130 (2013).
[26]J. Liu, J. Ni, Y. Zhao, H. Wang, L. Gao, J. Mater. Chem. A, 1, 12879 (2013).
[27]P. Wu, N. du, H. Zhang, J. Yu, D. Yang, J. Phys. Chem. C, 115, 3612 (2011).
[28]C. Ban, Z. Wu, D.T. Gillaspie, L. Chen, F. Yan, J.L. Blackburn, A.C. Dillon, Adv. Mater., 22, E145 (2010).